Molecular Engineering of Stilbazolium Derivatives for Second-Order Nonlinear Optics

Zhou Yang,*,† Mojca Jazbinsek,† Blanca Ruiz,† Shanmugam Aravazhi,† Volker Gramlich,‡ and Peter Günter†

Nonlinear Optics Laboratory, Institute of Quantum Electronics, and Laboratory of Crystallography, ETH Hönggerberg, CH-8093 Zürich, Switzerland

Received March 20, 2007. Revised Manuscript Received May 7, 2007

Three series of ionic stilbazolium salts with different counteranions have been synthesized to investigate the effect of counteranion size to crystal packing. Single crystals of five new salts were successfully grown from solution by the slow cooling and slow evaporation techniques. X-ray studies revealed that three of them show the triclinic space group *P*1 and two crystallize in the monoclinic space group *Cc* and $P2_1/c$, respectively. Kurtz powder tests revealed that out of the eight new stilbazolium salts, six possess noncentrosymmetric structures and three show large powder second-harmonic generation efficiencies higher or similar to that of 4-*N*,*N*-dimethylamino-4′-*N*′-methyl-stilbazolium tosylate (DAST). The optimal crystalline packing for electro-optics with perfectly aligned chromophores was achieved in three of the investigated compounds. The reasons for considerably different macroscopic nonlinearities of these compounds have been explored in terms of intermolecular interactions.

1. Introduction

There has been a continuing effort to develop organic materials with large second-order optical nonlinearities because of their potential for various applications in THz imaging and spectroscopy, telecommunications, optical information processing, and optical data storage.[1−7] Organic nonlinear optical materials have been shown to offer very fast response with modulation frequencies above 1 THz[8] and very high electro-optical and nonlinear optical coefficients compared to inorganic standards.[9,10] Single crystals are among the most attractive materials because of their typically large macroscopic nonlinearities, high packing densities, and superior long-term orientational and photochemical stabilities as well as their optical quality compared to poled polymers.[4,5] In addition to a large first-order hyperpolarizability (β) of the molecules used in this study, the macroscopic second-order susceptibilities ($\chi^{(2)}$) are strongly dependent on the relative arrangement and orientation of the π-conjugated chromophores in the crystalline lattice. However, considering that roughly 75% of the nonchiral organic compounds crystallize centrosymmetrically and thus exhibit no macroscopic second-order optical nonlinearity,[6] the noncentrosymmetric orientation of the chromophores in the bulk is one of the most important issues in developing useful and efficient second-order nonlinear optical crystalline materials. There have been several approaches utilized to artificially achieve noncentrosymmetry.[11−13] The use of strong coulomb interactions, for example, with a variation in counterions in stilbazolium salts has been demonstrated to be a simple and highly successful strategy to obtain materials with very large $\chi^{(2)}$.[12] DAST (4-*N*,*N*-dimethylamino-4′-*N*′-methyl-stilbazolium tosylate), with powder second harmonic generation efficiency of 1×10^3 times that of urea standard at 1907 nm, is one of the most well-known stilbazolium salts because of its large nonlinear optical susceptibility ($\chi^{(2)}$) and electro-optic coefficient (r).[14,15] Research has shown that DAST

* To whom correspondence should be addressed. E-mail: zhouyang@phys.ethz.ch.

† Nonlinear Optics Laboratory, Institute of Quantum Electronics, ETH Hönggerberg.

‡ Laboratory of Crystallography, ETH Hönggerberg.

(1) Bosshard, Ch.; Bösch, M.; Liakatas, I.; Jäger, M.; Günter, P. In *Nonlinear Optical Effects and Materials*; Günter, P., Ed.; Springer-Verlag: Berlin, 2000.
(2) *Molecular Nonlinear Optics: Materials, Physics, and Devices*; Zyss, J., Ed.; Academic Press: New York, 1994.
(3) Nalwa, H. S.; Miyata, S. *Nonlinear Optics of Organic Molecules and Polymers*; CRC Press: Boca Raton, FL 1997.
(4) Meredith, G. R. In *Nonlinear Optical Properties of Organic and Polymeric Materials*; Williams, D. J., Ed.; ACS Symposium Series Vol. 233; American Chemical Society: Washington, DC, 1983; pp 27−56.
(5) Coe, B. J.; Harris, J. A.; Asselberghs, I.; Wostyn, K.; Clays, K.; Persoons, A.; Brunschwig, B. S.; Coles, S. J.; Gelbrich, T.; Light, M. E.; Hursthouse, M. B.; Nakatani, K. *Adv. Funct. Mater*. **2003**, *13*, 347.
(6) Nicoud, J. F.; Twieg, R. J. *Nonlinear Optical Properties of Organic Molecules and Crystals*; Chemla, D. S., Zyss, J., Eds.; Academic Press, Orlando, FL, 1987; Vol. 1, pp 227−296.
(7) Li, D.; Ratner, M. A.; Marks, T. J.; Zhang, C.; Yang, J.; Wong, G. K. *J. Am. Chem. Soc*. **1990**, *112*, 7389.
(8) Hochberg, M.; Baehr-Jones, T.; Wang, G. X.; Shearn, M.; Harvard, K.; Luo, J. D.; Chen, B. Q.; Shi, Z. W.; Lawson, R.; Sullivan, P.; Jen, A. K. Y.; Dalton, L.; Scherer, A. *Nat. Mater*. **2006**, *5*, 703−709.
(9) Cheng, Y. J.; Luo, J. D.; Hau, S.; Bale, D. H.; Kim, T. D.; Shi, Z. W.; Lao, D. B.; Tucker, N. M.; Tian, Y. Q.; Dalton, L. R.; Reid, P. J.; Jen, A. K. Y. *Chem. Mater*. **2007**, *19*, 1154.
(10) Kim, T. D.; Kang, J. W.; Luo, J. D.; Jang, S. H.; Ka, J. W.; Tucker, N.; Benedict, J. B.; Dalton, L. R.; Gray, T.; Overney, R. M.; Park, D. H.; Herman, W. N.; Jen, A. K. Y. *J. Am. Chem. Soc*. **2007**, *129*, 488.
(11) Nemoto, N.; Abe, J.; Miyata, F.; Shirai, Y.; Nagase, Y. *J. Mater. Chem*. **1997**, *7*, 1389.
(12) Marder, S. R.; Perry, J. W.; Schaefer, W. P. *Chem. Mater*. **1994**, *6*, 1137.
(13) Kwon, O. P.; Ruiz, B.; Choubey, A.; Mutter, L.; Schneider, A.; Jazbinsek, M.; Gramlich, V.; Günter, P. *Chem. Mater*. **2006**, *18*, 4049.
(14) Marder, S. R.; Perry, J. W.; Schaefer, W. P. *Science* **1989**, *245*, 626.
(15) Pan, F.; Wong, M. S.; Bosshard, Ch.; Günter, P. *Adv. Mater*. **1996**, *8*, 592.

10.1021/cm070764e CCC: $37.00
Published on Web 06/09/2007

promises to work well for highly efficient and high-speed electro-optic applications[16−18] as well as THz generation and detection.[19,20] However, theoretical calculations suggest that the macroscopic susceptibilities of crystalline materials based on donor−acceptor disubstituted stilbenes have by far not reached the upper limits yet.[1] In addition, the growth of highly nonlinear optical quality bulk or thin films of DAST crystals still remains a big challenge;[21,22] therefore, novel materials with nonlinear properties similar to those of DAST but with superior growth possibilities are greatly desired.

Much effort has been directed toward developing new molecules with high molecular nonlinearities that would promote better noncentrosymmetric crystal packing and enable easier and faster bulk crystal growth.[23−25] In our previous study, we have found that minor modification of substituents on the counteranion can considerably change the crystal structure and second harmonic generation (SHG) activity of stilbazolium salts.[25,26] Furthermore, we have also found that other than the general counter anions like tosylate, bulky counteranions such as naphthalenesulfonate can induce a noncentrosymmetric structure with an even higher SHG efficiency.[27]

In the present investigation, three series of stilbazolium derivatives with various sizes of the counter anions have been systematically investigated to understand the effect of counteranions on the crystal structure and SHG activity of these compounds. Together with the two recently developed salts,[26,27] six other new stilbazolium derivatives have been designed, synthesized, and crystallized. Out of the eight investigated salts, six possess noncentrosymmetric structures and three SHG activities higher or similar to that of DAST.

2. Experimental Section

Synthesis. *General Considerations.* All reagents were purchased as high purity from Aldrich and used without further purification. ^{1}H NMR spectra were recorded on a Brucker 300 MHz spectrometer on DMSO-d_6 solutions. UV−vis spectra were recorded by a Perkin-Elmer Lambda 9 spectrometer. Elemental analyses were performed by the Microanalytical Laboratory, ETH. Thermal analysis was conducted on a Perkin-Elmer TGA-7 and DSC-7 spectrometer at a heating rate of 10 °C/min.

All salts were synthesized via metathesization of the iodide salt with the sodium salt of the corresponding anion, as described previously.[12] Sodium salt of 2,4,6-trimethyl-benzenesulfonic acid was obtained by reaction of 2,4,6-trimetheylbenzenesulfonate acid with equivalent NaOH. Purification was done by recrystallization from methanol or DMF for three times. The products were dried in a vacuum for 24 h to remove solvents before characterizing them by NMR and elemental analysis.

4-N,N-Dimethylamino-4′-N′-methyl-stilbazolium 2,4-dimetheyl-benzenesulfonate, DSDMS. Yield: 55%. ^{1}H NMR (300 MHz, DMSO-d_6): δ 8.69 (d, 2H, J = 7.2 Hz, C_5H_4N), 8.05 (d, 2H, J = 6.9 Hz, C_5H_4N), 7.93 (d, 1H, J = 16.2 Hz, CH), 7.60 (d, 2H, J = 9.0 Hz, C_6H_4), 7.59 (d, 1H, J = 7.8 Hz, $C_6H_4SO_3^-$), 7.19 (d, 1H, J= 16.2 Hz, CH), 6.92 (t, 2H, J = 11.7 Hz, $C_6H_4SO_3^-$), 6.80 (d, 2H, J = 9.0 Hz, C_6H_4), 4.17 (s, 3H, NMe), 3.02 (s, 6H, NMe_2), 2.47 (s, 3H, Me), 2.36 (s, 3H, Me). C, H, N anal. Calcd for $C_{24}H_{28}N_2O_3S$: C, 67.90; H, 6.65; N, 6.60. Found: C, 67.90; H, 6.81; N, 6.67.

4-N,N-Dimethylamino-4′-N′-methyl-stilbazolium 1-naphthalene-sulfonate, DSNS-1, Yield: 68%. ^{1}H NMR (300 MHz, DMSO-d_6): δ 8.85 (t, 1H, J = 9.9 Hz, $C_{10}H_7SO_3^-$), 8.68 (d, 2H, J = 6.6 Hz, C_5H_4N), 8.04 (d, 2H, J = 6.9 Hz, C_5H_4N), 7.94−7.85 (m, 4H, $C_{10}H_7SO_3^-$ + CH), 7.60 (d, 2H, J = 9.0 Hz, C_6H_4), 7.50−7.40 (m, 3H, $C_{10}H_7SO_3^-$), 7.18 (d, 1H, J = 16.2 Hz, CH), 6.79 (d, 2H, J = 9.0 Hz, C_6H_4), 4.16 (s, 3H, NMe), 3.02 (s, 6H, NMe_2). C, H, N anal. Calcd for $C_{26}H_{26}N_2O_3S$: C, 69.93; H, 5.87; N, 6.27. Found: C, 69.64; H, 6.12; N, 6.18.

4-N,N-Dimethylamino-4′-N′-methyl-stilbazolium 4-amino-1-naph-thalenesulfonate, DSANS. Yield: 71%. ^{1}H NMR (300 MHz, DMSO-d_6): δ 8.73−8.70 (m, 1H, $C_{10}H_6SO_3^-$), 8.68 (d, 2H, J = 6.9 Hz, C_5H_4N), 8.04−8.01 (m, 3H, C_5H_4N + $C_{10}H_6SO_3^-$), 7.92 (d, 1H, J = 16.2 Hz, CH), 7.66 (d, 1H, J = 7.8 Hz, $C_{10}H_6SO_3^-$), 7.60 (d, 2H, J = 8.7 Hz, C_6H_4), 7.39−7.33 (m, 2H, $C_{10}H_6SO_3^-$), 7.18 (d, 1H, J = 16.2 Hz, CH), 6.79 (d, 2H, J = 9.0 Hz, C_6H_4), 6.52 (d, 1H, J = 7.8 Hz, $C_{10}H_6SO_3^-$), 5.81 (s, 2H, NH_2), 4.16 (s, 3H, NMe), 3.02 (s, 6H, NMe_2). C, H, N anal. Calcd for $C_{26}H_{27}N_3O_3S$: C, 67.66; H, 5.90; N, 9.10. Found: C, 67.64; H, 5.90; N, 9.13.

4-N,N-Dimethylamino-4′-N′-methyl-stilbazolium 4-styrenesulfonate, DSSS. Yield: 64%. ^{1}H NMR (300 MHz, DMSO-d_6): δ 8.69 (d, 2H, J = 6.9 Hz, C_5H_4N), 8.04 (d, 2H, J = 6.6 Hz, C_5H_4N), 7.93 (d, 1H, J = 16.2 Hz, CH), 7.60−7.54 (m, 4H, $C_6H_4SO_3^-$, 7.42 (d, 2H, J = 8.7 Hz, C_6H_4), 7.19 (d, 1H, J = 16.2 Hz, CH), 6.80 (d, 2H, J = 9.0 Hz, C_6H_4), 6.73 (t, 1H, J = 17.7 Hz, CH), 5.69 (d, 1H, J = 18.3 Hz, CH_2), 5.28 (d, 1H, J = 12.0 Hz, CH), 4.17 (s, 3H, NMe), 3.02 (s, 6H, NMe). C, H, N anal. Calcd for $C_{24}H_{26}N_2O_3S$: C, 68.22; H, 6.20; N, 6.63. Found: C, 67.96; H, 6.18; N, 6.68.

4-N,N-Dimethylamino-4′-N′-methyl-stilbazolium diphenylamno-4-sulfonate, DSPAS. Yield: 52%. ^{1}H NMR (300 MHz, DMSO-d_6): δ 8.69 (d, 2H, J = 6.6 Hz, C_5H_4N), 8.23 (s, 1H, NH), 8.04 (d, 2H, J = 6.9 Hz, C_5H_4N), 7.92 (d, 1H, J = 15.9 Hz, CH), 7.60 (d, 2H, J = 9.0 Hz, C_6H_4), 7.44 (d, 2H, J = 8.4 Hz, $C_6H_4SO_3^-$), 7.25−7.13 (m, 3H, C_6H_5 + CH), 7.08 (d, 2H, J = 7.5 Hz, C_6H_5), 6.97 (d, 2H, J = 8.7 Hz, $C_6H_4SO_3^-$), 6.82−6.77 (m, 3H, C_6H_5 + C_6H_4), 4.16 (s, 3H, NMe), 3.02 (s, 6H, NMe). C, H, N anal. Calcd for $C_{28}H_{29}N_3O_3S$: C, 68.97; H, 5.99; N, 8.62. Found: C, 68.31; H, 6.05; N, 8.45.

4-N,N-Dimethylamino-4′-N′-methyl-stilbazolium Methyl Orange, DSMO. Yield: 56%. ^{1}H NMR (300 MHz, DMSO-d_6): δ 8.69 (d, 2H, J = 6.9 Hz, C_5H_4N), 8.04 (d, 2H, J = 7.2 Hz, C_5H_4N), 7.92 (d, 1H, J = 16.2 Hz, CH), 7.81 (d, 2H, J = 9.3 Hz, $C_6H_4SO_3^-$), 7.71 (s, 4H, $C_6H_4N_2$), 7.60 (d, 2H, J = 9.0 Hz, C_6H_4), 7.19 (d, 1H, J = 16.2 Hz, CH), 6.85 (d, 2H, J = 9.3 Hz, $C_6H_4SO_3^-$), 6.80 (d,

(16) Geis, W.; Sinta, R.; Mowers, W.; Deneault, S. J.; Marchant, M. F.; Krohn, K. E.; Spector, S. J.; Calawa, D. R.; Lyszczarz, T. M. *Appl. Phys. Lett.* **2004**, *84*, 3729−3731.
(17) Cai, B.; Ushiwata, T.; Komatsu, K.; Kaino, T. *Jpn. J. Appl. Phys.* **2004**, *43*, L390.
(18) Pan, F.; McCallion, K.; Chiappetta, M. *Appl. Phys. Lett*. **1999**, *74*, 492.
(19) Adachi, H.; Taniuchi, T.; Yoshimura, M.; Brahadeeswaran, S.; Higo, T.; Takagi, M.; Mori, Y.; Sasaki, T.; Nakanishi, H. *Jpn. J. Appl. Phys.* **2004**, *43*, L1121.
(20) Schneider, A.; Biaggio, I.; Günter, P. *Appl. Phys. Lett.* **2004**, *84*, 2229−2231.
(21) Thakur, M.; Titus, J.; Mishra, A. *Opt. Eng*. **2003**, *42*, 456.
(22) Hosokawa, Y.; Adachi, H.; Yoshimura, M.; Mori, Y.; Sasaki, T.; Masuhara, H. *Cryst. Growth Des*. **2005**, *5*, 861.
(23) Wong, M. S.; Pan, F.; Bosch, M.; Spreiter, R.; Bosshard, Ch.; Günter, P. *J. Opt. Soc. Am*. **1998**, *15*, 426.
(24) Okada, S.; Nogi, K.; Anwar; Tsuji, K.; Duan, X-M.; Oikawa, H.; Matsuda, H.; Nakanishi, H. *Jpn. J. Appl. Phys.* **2003**, *42*, 668.
(25) Yang, Z.; Aravazhi, S.; Schneider, A.; Seiler, P.; Jazbinsek, M.; Günter, P. *Adv. Funct. Mater.* **2005**, *15*, 1072.
(26) Yang, Z.; Mutter, L.; Ruiz, B.; Aravazhi, S.; Stillhart, M.; Jazbinsek, M.; Gramlich, V.; Günter, P. *Adv. Funct. Mater.* **2007**, in press.
(27) Ruiz, B.; Yang, Z.; Jazbinsek, M.; Gramlich, V.; Günter, P. *J. Mater. Chem.* **2006**, *16*, 2839.

Table 1. Melting Points and Powder SHG Efficiencies of the Investigated Compounds

series 1	melting point (°C)	powder SHG[a]	series 2	melting point (°C)	powder SHG[a]	series 3	melting point (°C)	powder SHG[a]
DAST	256 ± 1	1.0	DSNS-1	>300	0.7	DSSS	266 ± 1	1.0
DSDMS	267 ± 1	0.7	DSNS-2	>300	1.5	DSPAS	241 ± 1	0.1
DSTMS	258 ± 1	1.0	DSANS	263 ± 1	0	DSMO	269 ± 1	0

[a] 1907 nm fundamental radiation, compared with DAST.

Table 2. Crystallographic Data for Stilbazolium Derivatives

	DSNS-1	DSNS-2	DSANS	DSDMS	DSTMS	DAST
formula	$C_{26}H_{26}N_2O_3S$	$C_{26}H_{26}N_2O_3S$	$C_{26}H_{27}N_3O_3S$	$C_{24}H_{28}N_2O_3S$	$C_{25}H_{30}N_2O_3S$	$C_{23}H_{26}N_2O_3S$
FW	446.55	446.55	461.59	424.54	438.57	410.52
cryst syst	triclinic	triclinic	monoclinic	triclinic	monoclinic	monoclinic
space group	*P*1	*P*1	$P2_1/c$	*P*1	*Cc*	*Cc*
a (Å)	7.559(1)	7.864(4)	9.521(2)	7.685(2)	10.266(1)	10.365(3)
b (Å)	8.813(1)	8.054(4)	14.068(3)	8.056(2)	12.279(1)	11.322(4)
c (Å)	9.852(2)	9.893(5)	17.012(3)	9.797(2)	17.963(2)	17.892(4)
α (deg)	71.32(1)	70.04(5)		70.50(2)		
β (deg)	69.34(1)	73.31(5)	103.26(1)	70.11(2)	93.04(1)	92.24(2)
γ (deg)	68.98(1)	83.69(5)		80.30(2)		
V (Å^3)	558.9(2)	564.1(5)	2217.8(7)	542.4(2)	2261.2(3)	2098.2(11)

2H, J = 9.0 Hz, C_6H_4), 4.17 (s, 3H, NMe), 3.06 (s, 6H, NMe), 3.02 (s, 6H, NMe). C, H, N anal. Calcd for $C_{30}H_{33}N_5O_3S$: C, 66.28; H, 6.12; N, 12.88. Found: C, 66.11; H, 6.15; N, 12.86.

SHG Measurements. To determine the SHG efficiency, we used 150 fs pulses at wavelength λ = 1907 nm from an optical parametrical amplifier pumped by an amplified Ti:sapphire laser as the pump wave. The measurements were carried out as described previously.[25] After grinding, the microcrystalline powdered samples were sieved to a particle size distribution of 63−90 μm and squeezed into a 1.00 mm Hellma UV quartz sample cell to give a constant sample thickness. The SHG signals were calibrated with respect to 63−90 μm powdered DAST samples.

Crystal Growth. The slow cooling and slow evaporation solution growth techniques were adapted for the growth. Slow cooling experiments were performed as described previously,[25] mainly using methanol as solvent. The slow evaporation experiments were carried out with three different solvents: methanol, DMF, and DMSO according to the solubility of our materials in these solvents. Different vessels have been used for crystal growth with different solvents. An evaporating dish was used for DMF and a flask was used for methanol. For DMSO, droplets of the solution were placed between glass plates and left to slowly evaporate at 50 °C.

X-ray Crystallography. The crystal structures were measured on X-ray diffractometers equipped with CCD detectors and solved and refined with SHELX. For details see the Supporting Information. Crystallographic data for DSNS-1, DSNS-2, DSANS, DSSMS, DSTMS, and DAST are presented in Table 2.

3. Results and Discussion

3.1. Design and Synthesis.

Previous studies of our group[23,25] and Nakanishi et al.[24] have provided important information on how a change of the counteranion will change the crystal structure and SHG activity of stilbazolium salts, thus offering almost unlimited design possibilities to obtain new materials by straightforwardly varying counter anions. On the other hand, however, the chromophore packing and crystal growth cannot be reliably predicted.[4] Therefore, we had to rely on an experimental approach in order to identify the main factors that lead to optimized crystalline packing.

In this work, we report on the results of three series and eight new stilbazolium salts as shown in Scheme 1. The first series includes DAST derivatives by adding methyl groups on the tosylate anion of DAST. The second and third series include bulky counteranions, whose sizes are bigger than those of the first series along the long axis of the whole molecule (series 3) or the direction vertical to that (series 2).

Scheme 1. Structures of the Stilbazolium Derivatives and Their Abbreviations

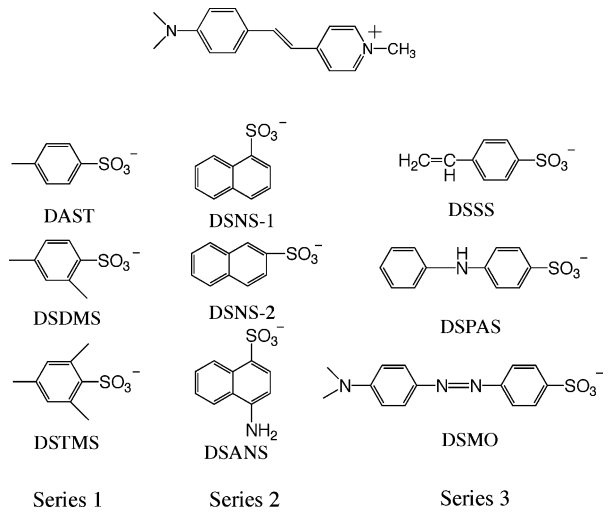

3.2. Characterization and Powder Nonlinear Optical Studies.

The results of the melting points and powder second harmonic generation (SHG) measurement of these compounds are summarized in Table 1.

From the table, we can see that all of the eight new compounds have melting points similar to DAST (256 ± 1) °C except of DSNS-1 and DSNS-2. Both of these compounds are tightly bound and have melting points higher than 300 °C. The high thermal stability of naphthalenesulfonate should be the determining factor for their high melting temperatures. In the case of the last compound in the series, DSANS, the presence of the amino group on naphthalenesulfonate reduces its melting point to about 263 °C.

As a preliminary test of their nonlinear optical activity, we have carried out powder SHG studies to measure the activities of these compounds and compare them with DAST, the state-of-the-art organic nonlinear optical crystal. For these

experiments, the Kurtz powder technique[28] was used with a setup as described in ref 25. The pump wave, from an optical parametric amplifier pumped by an amplified Ti:Sapphire femtosecond laser, with a wavelength of 1907 nm, was used to avoid absorption of the harmonic signals. For the SHG conversion efficiencies measurement, we used material that has been sieved to a same particle size distribution (63−90 nm). Out of the eight compounds synthesized, six exhibited second harmonic signals, out of which five show strong SHG efficiencies comparable to DAST (Table 1). The SHG efficiencies of DSDMS and DSNS-1 are about 0.7 times as the one of DAST, and the efficiencies of DSTMS and DSSS are quite similar to DAST. The SHG efficiency of DSNS-2 is 1.5 times the one found in DAST and among the largest powder SHG efficiencies measured so far.

Comparing the SHG activity of the three series of materials, we see that all of the three compounds of series 1 exhibit strong second harmonic signals. This indicates that tosylate is not the only counteranion to favor large SHG activity. Minor modification of the counteranion can produce novel stilbazolium derivatives with favorable noncentrosymmetric packing arrangement considering that the counter anions of DSDMS and DSTMS were obtained by adding one or two methyl groups on the tosylate of DAST, respectively. Moreover, it implies that the second-order nonlinear optical activity of DAST can be further optimized by changing the counter anions. In series 2, the counter anions contain naphthalene ring compared to phenyl ring of series 1. By using 2-naphthalenesulfonate as a counteranion (DSNS-2), the powder SHG efficiency measured is 50% higher than that of DAST. This is, to the best of our knowledge, the only stilbazolium derivative with a considerably higher macroscopic second-order nonlinearity than DAST. Using a relatively large counteranion compared to tosylate of DAST can therefore induce a noncentrosymmetric structure with a very high SHG activity. For the series 3, only DSSS shows strong SHG efficiency comparable to DAST and further increasing of the counteranion size like for DSPAS and DSMO does not lead to a favorable packing arrangement. We can conclude that using such long counteranions is not favorable to yield high second-order nonlinear optical effects.

3.3. Crystal Growth. The slow cooling and slow evaporation solution growth techniques have been used to grow single crystals of these new stilbazolium salts.

DSDMS and DSTMS can be well-dissolved in alcohol, especially in methanol.[15] Therefore, methanol was identified as the most suitable solvent for the growth of DSDMS and DSTMS crystals. From the solubility measurement, we learned that the solubility of DSTMS in methanol is around two times the one measured for DAST at the same temperature.[26] The slow cooling technique was adapted first for the growth of DSTMS crystals. It was found that DSTMS crystals appear as red thin plates and continue to grow preferentially along all edges in all directions in contrast to DAST, which preferentially grows along the polar axis [100].[29] Bulk DSTMS single crystals with dimensions of 33 × 33 × 2 mm^3 have been grown for future nonlinear optical measurement (Figure 1a). For DSDMS, the slow evaporation technique[30] at a constant temperature was adopted because we found that its solubility is mainly sensitive to the amount of the solvent and almost independent of temperature. Bulk single crystals with dimensions of 10 × 2 × 0.2 mm^3 have been obtained in 2−3 weeks (Figure 1b).

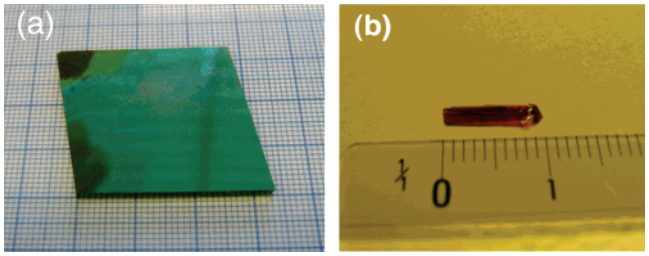

Figure 1. Single crystal of DSTMS (a) and DSDMS (b).

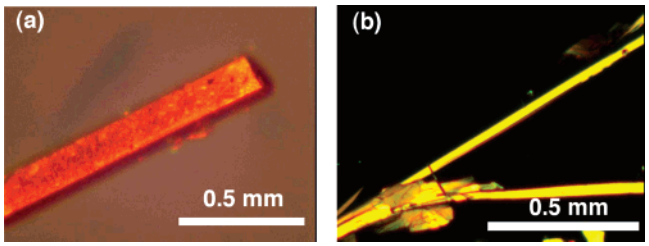

Figure 2. (a) Crystal of DSNS-1 and (b) crystals of DSNS-2 grown by slow evaporation as observed between the crossed polarizers in a microscope.

The solubility of the second group of materials in methanol was too low to obtain single crystals. Thus dimethylformamide (DMF) and dimethylsulfoxide (DMSO) have been used for the crystal growth. Both DSNS-1 and DSANS single crystals with lengths of about 2 mm were obtained by slow evaporation from DMF in 2−3 weeks. Figure 2a) shows DSNS-1 crystal that was placed between crossed polarizers in a polarizing microscope. A perfect rodlike single crystal could be seen from the microscope. For DSNS-2, DMSO was found to be a very good solvent. Single crystals were obtained from this solvent both by slow evaporation and slow cooling techniques.[27] Using the slow evaporation technique, 2 mm long thin square needlelike crystals with dimension of a few tens of micrometers were obtained (Figure 2b). The slow cooling technique yielded platelike crystals with a size of about 0.5 mm.[27]

In the third series of materials, DSPAS is very easily dissolved in methanol and ethanol; however, only crystalline powder could be obtained using either the slow cooling or slow evaporation techniques. In the case of DSSS and DSMO, only polycrystalline material could be obtained by the slow evaporation technique, even through both materials are well-dissolved in DMF.

Comparing the crystal growth results of the three series of materials, we can find that compounds of series 1 nucleated much easier than those of series 2 and series 3. Bulk crystals of series 1 with dimensions on the order of 1

(28) Kurtz, S. K.; Perry, T. T. *J. Appl. Phys.* **1968**, *39*, 3798.

(29) Manetta, S.; Ehrensperger, M.; Bosshard, C.; Günter. P. *C. R. Phys.* **2002**, *3*, 449.

(30) Bosshard, Ch.; Sutter, K.; Prêtre, Ph.; Hulliger, J.; Flörsheimer, M.; Kaatz, P.; Günter, P. *Organic Nonlinear Optical Materials*; Gordon and Breach Publisher: London, 1995.

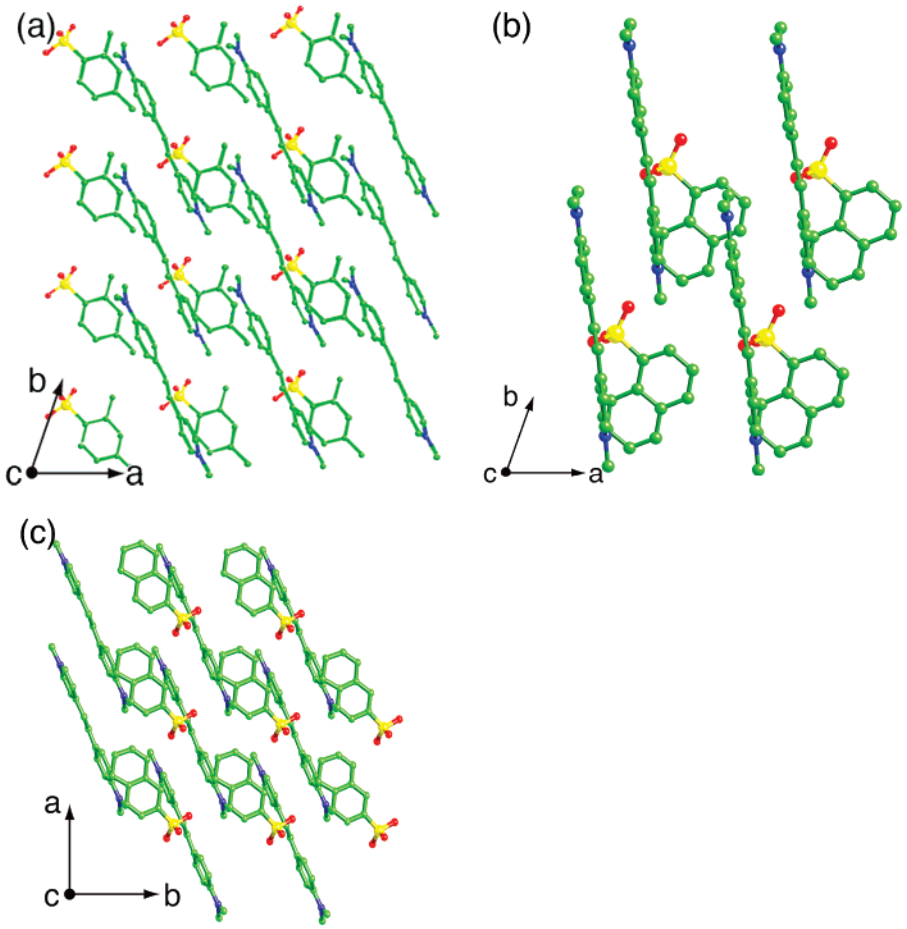

Figure 3. Crystal structure of (a) DSDMS, (b) DSNS-1, and (c) DSNS-2 with triclinic *P*1 symmetry viewed along the *c*-axis.

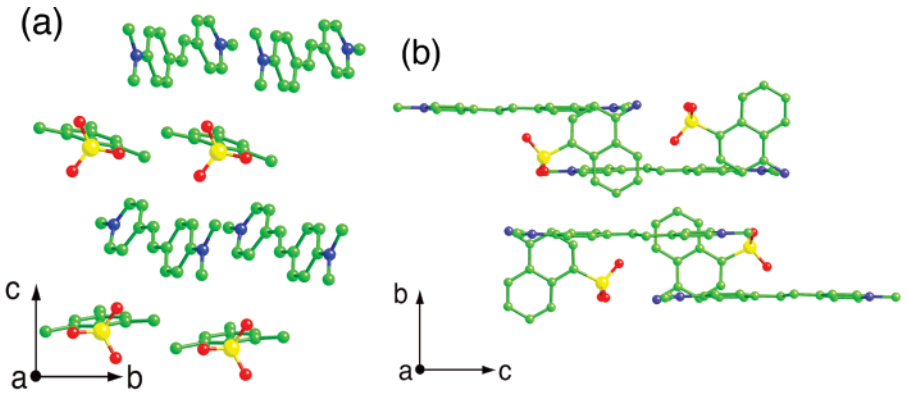

Figure 4. Crystal packing diagrams: (a) DSTMS with a monoclinic *Cc* symmetry and (b) DSANS with a monoclinic $P2_1/c$ symmetry viewed along the *a*-axis.

cm can be grown from methanol. Compounds of series 2 can be grown in single crystalline form up to 1−2 mm length; they are all considerably smaller than those of series 1. In series 3, however, no single crystals could be grown, although some of the compounds exhibited a very good solubility. The presented results suggest that when bulky counteranions are used, nucleation tends to be suppressed. Moreover, introducing especially long counteranions in stilbazolium derivaties results in a poor crystal growth, at least in the case of DSPAS and DSMO.

The optical quality of all crystals has been investigated by placing them between crossed polarizers in a microscope. Rotation of the crystal around the direction of light propagation allowed complete and homogeneous extinction when the indicatrix axis (or its projection to the plane of the crystal plate) was aligned parallel to the polarization of the transmitted light. This indicates that the crystals are single crystalline. For polycrystalline materials, some parts appear transparent and others opaque when rotating the samples.

3.4. X-ray Crystallographic Study. Single-crystal X-ray analysis was carried out in DSDMS, DSTMS, DSNS-1, DSNS-2, and DSANS crystals. Crystallographic data are listed in Table 2, where DAST is added for comparison. The crystal packing diagrams for the structures of the studied crystals are presented in Figures 3 and 4. The crystal structures of DSDMS, DSNS-1, and DSNS-2 are triclinic, having space group symmetry *P*1 with one ion pair per unit cell. The three-dimensional packing exhibits alternating

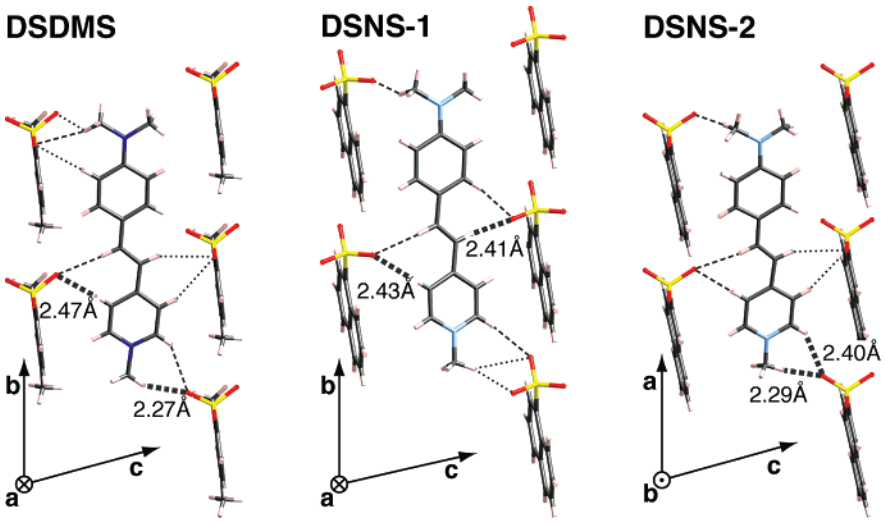

Figure 5. Stilbazolium chromophore environment for three investigated compounds having a triclinic *P*1 structure with all chromophores perfectly parallel: DSDMS, DSNS-1, and DSNS-2, projected along *a*, *a*, and *b* crystallographic axes, respectively. The thick dashed lines represent hydrogen H···O bonds of <2.5 Å length (for these, the approximate lengths are given), the thin dashed lines represent hydrogen H···O bonds in the range of 2.5−2.7 Å, and the thin dotted lines represent hydrogen H···O bonds in the range of 2.7−2.9 Å.

acentric sheets of stilbazolium cations and counteranions. The observed parallel arrangement of all stilbazolium chromophores with the highest possible order parameter $<\cos^3\theta> = 1$ is a prerequisite for efficient electro-optic or second-order nonlinear optical effects. Therefore, high diagonal second-order nonlinear optical coefficients *d* and electro-optic coefficients *r* are expected for these crystals.[30]

The crystal structure of DSTMS (Figure 4a) is very similar to that of DAST, and also belongs to the monoclinic space group *Cc* (point group *m*, $Z = 4$). The sheets of cation chromophores are interleaved with sheets of counter anions. The planes of the counteranion rings are roughly perpendicular to the molecular planes of the cations. The tilting angle θ between the cation's long axis and the polar *a*-axis of the crystal is about 23°, giving an order parameter $<\cos^3\theta> = 0.78$ for the projection of molecular nonliearities to the polar axis. In the case of DAST, the θ value is about 20° ($<\cos^3\theta> = 0.83$).[14] Therefore, similar nonlinear optical characteristics are expected for DSTMS as for DAST, as also confirmed by the powder SHG test (see Table 1). Nonlinear optical measurement revealed that DSTMS possesses a high nonlinear optical susceptibility $\chi^{(2)}_{111} = 430 \pm 40$ pm/V at 1.9 μm.[26]

The space group symmetry of DSANS (Figure 4b) is monoclinic $P2_1/c$ and there are four ion pairs per unit cell. The cation chromophores are arranged almost parallel but packed in opposite directions. This is the only centrosymmetric structure among the five structures reported here. It is very interesting to note here that the powder SHG efficiency of DSANS raw material was about 2.0 times of that of DAST. After purifying, however, it crystallized centrosymmetrically and therefore showed no SHG activity. This means that the centrosymmetric structure of DSANS as reported here could be easily broken and transformed into noncentrosymmetric by introducing other materials, e.g., dopants. Introduction of additives during the growth or changing the growth conditions could therefore lead to new possibilities for the crystal engineering of highly nonlinear molecular salts, similar to nonlinear optical crystals based on weaker van der Waals and hydrogen bonds.[31]

3.5. Effect of Hydrogen Bonds. From the stilbazolium salts designed, we were able to obtain three (DSDMS, DSNS-1, and DSNS-2) that have a perfectly parallel alignment of the chromophores, which is optimal for maximizing the macroscopic electro-optic response of the material. According to the oriented-gas model,[32] these compounds should have a similar diagonal macroscopic nonlinearity of about $1/\cos^3(20°) \approx 1.2$ higher than that of DAST, in which the chromophores make an angle of about 20° with respect to the polar axis. The macroscopic nonlinearity of the new compounds was scanned by the powder SHG test (see Table 1). Because the powder size was much larger compared to the coherence length for SHG (in DAST, for example, this length is on the order of 1 μm), we expect that the powder test results can be considered quite relevant for estimating the macroscopic nonlinearity. Contrary to these expectations, we measured a powder test efficiency of DSNS-2 more than twice that of DSDMS and DSNS-1. We attribute this result to the intermolecular interactions that decrease the microscopic nonlinearity of chromophores in the solid state. In DAST, for example, it was shown that this effect decreases the macroscopic nonlinearity by as much as 80%,[33] which was attributed to strong coulomb interactions binding the chromophores with the counterions. Crystallographic data show that beside the coulombic interactions between the cation and anion parts, hydrogen bonds between the sulfonic oxygen atoms and double-bond hydrogen atoms also play a role in crystal packing and chromophore orientation. In DSTMS,[26] data shows that the hydrogen-bonded network is formed by two kinds of C−H···O hydrogen bonds between the cation layers and the anion layers with H···O distances of about 2.49 and 2.44 Å, respectively. Figure 5 shows the

(31) Kwon, O. P.; Jazbinsek, M.; Choubey, A.; Losio, P. A.; Gramlich, V.; Gunter, P.; *Cryst. Growth Des.* **2006**, *6*, 2327.
(32) Zyss, J.; Oudar, J. L. *Phys. Rev. A* **1982**, *26*, 2028.
(33) Bosshard, Ch.; Spreiter, R.; Günter, P. *J. Opt. Soc. Am. B* **2001**, *18*, 1620.

stilbazolium chromophore environment, i.e., the surrounding counter anions in the crystal structure, for DSDMS, DSNS-1, and DSNS-2, which all possess a *P*1 space group structure with perfectly parallel chromophores. We can clearly observe a weak hydrogen bond network that changes for different counterions. It is clear that the weak hydrogen bonds reduce the energy of the whole system and keep it more stable. However, its influence to microscopic and macroscopic nonlinearities may not be negligible. In fact, for DSNS-2 with macroscopic nonlinearities twice that of the other two compounds, we can see that the strongest hydrogen bonds appear at the end of the chromophore, whereas for DSDMS and DSNS-1, they appear rather in the π-conjugated bridge part of the chromophore, which might diminish the chromophore hyperpolarizability more seriously. Because the effect of the molecular environment is quite complex, more studies are needed to conclude whether the observed changes in nonlinearity of stilbazolium salts are due to the observed hydrogen bonds or coulomb interactions between the ionic parts. We can also see in Table 2 that the volume of the unit cell containing one stilbazolium chromophore and one counterion is the largest for DSNS-2 among the three *P*1 compounds. This results in a lower density of chromophores that should slightly reduce the nonlinearity. On the other hand, this means that the molecular units are further apart and the molecular hyperpolarizability less affected. The latter effect seems much more considerable and therefore future studies should also concentrate on possibilities to optimize the molecular environment in the ionic nonlinear optical salts in order to reach the theoretical limits.

4. Conclusions

We have investigated eight new stilbazolium salts, which have been grouped into three series with various sizes of the counter anions. The effect of the counteranions on the crystal structure and SHG activity of stilbazolium derivatives has been investigated by studying the growth, optical quality, SHG activity, and crystallographic structure of these new compounds. Out of the eight salts synthesized, six possess noncentrosymmetric structures and three possess SHG activity higher or similar to that of DAST. Comparison of the experimental results has shown that using especially long counteranions in stilbazolium derivatives not only suppresses the SHG activity but also inhibits the growth of single crystals. On the other hand, using a relatively bulk counteranion compared to tosylate of DAST has the possibility to induce a noncentrosymmetric structure with a higher SHG activity than that of DAST, even though a bulky counteranion may still cause difficulty of the compounds nucleation. A strong effect of intermolecular interactions such as hydrogen bonds on macroscopic nonlinearity of stilbazolium salts has been observed. Both the results of powder SHG measurement and crystal growth revealed that minor modification of tosylate can produce novel stilbazolium derivatives with high SHG efficiencies and improved crystal-growing characteristics.

Acknowledgment. We thank M. Stillhart for assistance with the powder test. This work has been supported by the Swiss National Science Foundation.

Supporting Information Available: Crystallographic information in text format. This material is available free of charge via the Internet at http://pubs.acs.org.

CM070764E